Astron. Astrophys. 335, 479–487 (1998)

ASTRONOMY AND ASTROPHYSICS

# Color distributions in E-S0 galaxies

## II. Evidence for diffuse dust concentration in the disks of disky E-type galaxies⋆

**R. Michard**

[1] Observatoire de la Cote d'Azur, Departement Augustin Fresnel B.P. 229, F-06304 Nice Cedex 4, France
[2] Observatoire de Paris, DEMIRM, 77 av. Denfert-Rochereau, F-75015 Paris, France

Received 14 November 1997 / Accepted 7 April 1998

**Abstract.** Reddening of the major axis compared to the minor axis on a given isophote, and asymmetry of the run of surface brightness and colour along the minor axis, are possible signatures of dust concentrated in the disk of an inclined two components galaxy, the first being somewhat ambiguous. From CFHT observations, these phenomena are shown to occur in nearly all disky ellipticals of sufficient flattening. They may also occur in the inner "decoupled" disks, appearing in some ellipticals both boxy and disky. HST frames in Lauer et al. (1995) for a few objects confirm the present findings.

Future modelling of diffuse dust in E classified galaxies should take into account this property of its distribution.

**Key words:** galaxies: elliptical and lenticulars, CD – galaxies: ISM – galaxies: fundamental parameters

### 1. Introduction

It is tempting to suppose that E galaxies contain, besides their local dust patches and lanes, a diffuse dust component more evenly distributed. Jura (1978), modelized the Rayleigh scattering from this dust, but Michard & Marchal (1991) were unable to detect the predicted polarization. On the other hand, the observation by IRAS of thermal dust emission in the far IR from many classical E-galaxies, implies significant amounts of dust (Jura et al., 1987; Knapp et al., 1989). The problem then arises to bring into a coherent picture the information about the dust in E-galaxies derived from IRAS and optical data. Contributions towards this goal have been published by de Jong et al (1990), Hansen et al. (1991), studying specific objects. An analysis of the transfer of stellar radiation through a dusty spherical galaxy by Witt et al. (1992) is also relevant.

A systematic study of the distribution of interstellar matter, both dust and gas, has been performed by Goudfrooij et al. (1994 a, b); the analysis of these data lead Goudfrooij (1995), Goudfrooij & de Jong (1995), to propose that the diffuse dust component might be responsible for the "dust mass discrepancy" between estimates based upon IRAS and optical data respectively, and could then play an important role in producing the observed colour gradients. The same conclusion is reached by Silva & Wise (1995), and Wise & Silva (1996).

The modelling of diffuse dust in E galaxies has been performed up to now for objects of spherical symmetry. This approximation is possibly adequate for spheroids, but it is not so for the many E-classified galaxies containing disks, i.e. the disky E's (diE). These are known to be similar to S0's, the distinction being *in part* due simply to a lesser inclination of the diE's, according to Michard (1994), but also to differences in disk-to-bulge ratio and dust content. In turn the S0's are similar to Sa's, without detected spiral pattern and with less interstellar dust. Recall that in Sa's the dust is concentrated in the disk. At a suitable projection, one side of the bulge along the minor axis is obscured and reddened. Michard & Simien (1993), or MS93, observed this *minor axis asymmetry* in a number of S0's, showed it to be colour dependent as expected for an effect of galaxian dust, and modeled the phenomenon with extended distributions of dust in an assumed thin disk.

The so-called "minor axis asymmetry" is seen only, for a given optical thickness of dust in the disk, in a limited range of inclination to the line of sight. For strictly edge-on objects, the asymmetry will disappear, and one will be left with an equatorial dust lane. At average inclinations, the asymmetry may become too small to show up, but the major axis is expected to remain somewhat redder than the minor axis along a given isophotal contour. This will also occur if the dust is concentrated *towards the equatorial plane*, although not necessarily in a thin layer.

We have searched for dust concentrated in the disk of disky E's, or perhaps towards their equatorial plane, using as observational tests primarily the minor axis asymmetry, and eventually the reddening of the major axis region as compared to the minor axis one. This second character is not however an unambiguous indication of the presence of dust, because it could also result of a difference in populations, and the corresponding colour gradients, between the bulge and the disk of two- component objects. Positive results have been found for a significant number of disky E's.

*Send offprint requests to*: R. Michard

⋆ Based on observations collected at the Canada-France-Hawaii Telescope and at the Observatoire du Pic du Midi

## 2. The data

### *2.1. Currently used notations*

1. boE, diE, unE: Subclasses of ellipticals, i.e. boxy, disky and undeterminate.
2. $a$, $c$, $r$ respectively major axis, minor axis and mean radius of the Reference Ellipse in the representation of an isophotal contour according to Carter (1978).
3. $q$, $\epsilon$ respectively axis ratio and ellipticity of the ellipse.
4. $e_i$, $f_i$ respectively cosine and sine harmonic coefficients of contour deviations from the Reference Ellipse.

### *2.2. Observational material*

#### 2.2.1. The Nieto sample

In 1989-91 the late J.L. Nieto and co-workers obtained, mostly at the CFHT, a collection of high resolution frames intended to study the core regions of E-classified galaxies. Preliminary results were published by Nieto et al. (1991a, b). Both B and Cousins R frames were available in many cases. For the study of colour distributions near the core, relatively nearby objects with $V_0 < 3000$ km/s were selected, in order to keep the full advantage of the available resolution. The "Nieto sample" thus formed encompasses 44 objects. The main characteristics of the frames are as follows:

1. CFHT observations, Dec 1989 and Apr 1990, for 22 sample galaxies. Cassegrain focus with scale 0.107 arcsec/pix and total field 641x1011 pixels. The galaxy was often away from the center of the field to get a PSF star inside the CCD target, so that the usable galaxian radius is between 10 and 30 arcsec.
2. CFHT observations, Apr and Jun 1991, for 20 sample galaxies, including 4 from the 1990 session. Prime focus with the HRcam, scale and total field as above. The HRcam observations are of lesser S/N ratio but the seeing is somewhat better. Same remark as above as regards the limiting radii.
3. Pic du Midi observations, Mar 1990, for 6 galaxies. Cassegrain focus of the 2m telescope with focal reducer, with scale 0.315 arcsec/pix and total field 320x512 pixels.
4. For the whole CFHT sample, the mean measured stellar FWHM were 0.72 arcsec in R and 0.85 in B. For the Pic du Midi subset, the corresponding values were 0.92 and 1.13 arcsec.

In the present paper, the Nieto sample will be used to search for evidence of dust concentration in the disks (or near the equatorial plane) of diE galaxies of sufficient inclinations to the line of sight.

#### 2.2.2. Data analysis techniques

These will be detailed in a forthcoming paper of this series. Only a summary of salient points is given below.

*Matching PSF's* Important errors can occur in colour measurements of the innermost regions of galaxies, due to differences in the PSF's of the two intercompared frames. This question has been studied by Vigroux et al. (1988), Franx et al. (1989), Peletier et al. (1990). We have performed many experiments about the effects of "differential seeing", notably upon the geometry of isochromes, designed more or less elaborate correction techniques, and tested their success with ad hoc models. Then *an operation of PSF matching has been systematically applied to the pairs of frames used for colour measurements*. These precautions, plus the rather good seeing of the CFHT frames, allows colour distributions to be measured up to the center of E-S0 galaxies. There are several cases of duplicate observations, where a given galaxy was observed twice with significantly different seeing conditions. The study of these cases indicate internal errors of 0.03 magnitude for these measurements near the center. However, sharply peaked colour distributions will be affected by the common limited resolution of the matched frames.

*Carter-like isophotal analysis* The isophotal analysis of the galaxian images (or at least the R image of the B,R pair), according to Carter's principles, is a necessary step in the applied reduction procedure. The set of *isophotes, in parametric form*, is then used to locate points in the galaxian image and measure the surface brightness, or in two images and measure a colour. The coordinates are the semi major axis $a$, or the mean radius $r$, of the Reference Ellipse in Carter's representation of isophotal contours and the eccentric anomaly $\omega$ along this ellipse. *Note that the "isophotes" here refered to, are not elliptical approximations, but retain the most useful details of the representation, i.e. the even harmonic coefficients*. They are however made symmetric about a fixed center, by cancelling the appropriate odd coefficients.

*1D colour measurements* A routine to measure separately the radial colour distribution along the minor axis and the major axis is available. The measurements are averaged along arcs of isophotes of 45 degrees extent in terms of the variable $\omega$. The two opposite halves of any axis are also measured separately.

A routine is also available to measure *the azimuthal colour distribution* in so called *isophotal rings*, that is bounded by *isophotal contours*, specified by the inner and outer radii of the corresponding Reference Ellipse. Here again isophotal contours are defined by the full Carter representation, symmetrized as noted above. The azimuthal colour distributions are quite effective in showing the presence of dust features, colour asymmetries, and of course differences in colour between the major axis and minor axis regions of an "isophotal ring".

*Minor axis asymmetries in the surface brightness* These characteristics asymmetries in the surface brightness distributions of inclined S0's were described in MS93. Frames of diE's were searched for this effect as explained in the quoted paper.

*2D displays* The peculiarities in the surface brightness and colour distributions giving evidence for dust concentration in the disk, or towards the equatorial plane, i.e. asymmetries in surface brightness and colour along the minor axis and/or a redder major axis, are of course seen in 2D displays. Maps of the colour index will show differences between isochromes and isophotes, with the former being flatter and somewhat displaced along the minor axis.

*These appearances may unfortunately be influenced by various causes of errors! A flattening of isochromes may be induced by imperfect PSF matching. Their displacement may result from imperfect superposition of the galaxian centers in the two frames*. It will also produce asymmetries in 1D colour profiles.

The effects of such errors have been studied from a consideration of the pseudo-colours $B-B$ or $R-R$ from pairs of frames taken in the same observing conditions and with similar S/N ratios. Such a duplication of the data was not very frequent, half a dozen cases or less for each of the CFHT set-ups. Now, $B-B$ or $R-R$ maps should be flat: the effects of noise, poor PSF matching or poor alignment are readily recognized. In particular, poor alignment gives rise to asymmetries in the innermost range of radii, an effect rather distinct from the appearances of the isochromes in Figs. 5-11. To sum up, although the effects of poor alignement and poor PSF matching cannot be absent from the present data, they are not such as to affect the results.

Remark: From experiments with purposely biased frame alignments, it may be estimated that the superposition of pairs of frames was obtained with an accuracy of 0.01 arcsec (worse for objects with a broad core).

## 3. Results

### *3.1. Discussion of criteria for "dust in the disk"*

*The phenomenon of minor axis asymmetry* seems to be a safe indication of the presence of dust concentration near the equatorial plane of an oblate object, or the disk of a two component galaxy (see MS93). Unfortunately, the asymmetries can be detected only in a limited range of inclinations, and are easily masked by faint dust patterns. As noted above, they are also affected by small errors in defining the galaxian center. It is of course necessary to check that the asymmetries in surface brightness and colour are coherent: the red side of a disky flattened galaxy should also be the obscured one.

*A redder colour along the major axis* than along the minor axis of successive isophotes, can be due to dust concentration in the equatorial plane of an ellipsoidal or two-component galaxy, also when no asymmetry is detected perhaps due to unappropriate inclination. In this case, the isochromes may become much flatter than the isophotes.

A similar effect can also be produced, for the latter kind of objects, by a difference between the population, and the corresponding colour gradients, of the bulge and disk respectively. In the extreme case of an edge-on galaxy with a "razor blade" disk, one would find along the minor axis the strong colour gradient usually found in bulges, while the major axis would be dominated by the colour gradient of the disk population. If this gradient is much smaller than the one of the bulge, the isochromes may again become much flatter than the isophotes.

The two situations can be distinguished, at least to some extent. An equatorial dust layer will affect the colours of the inner spheroid, so that the flattening of the isochromes will be apparent in the central regions of the galaxy. A difference in the colours gradients of the spheroid and disk, on the other hand, will not affect the isochromes in the central "bulge dominated" region; their flattening will appear progressively outwards, as the disk becomes more influential in the light and colour distributions. Fig. 1 displays the two situations from ad hoc numerical experiments, involving the same $r^{1/4}$ spheroid, with a colour gradient $\Delta C/\Delta \log r$=0.1. In one case, a stellar, dustless, exponential disk, with $\epsilon$=0.74 and *of constant colour* was added. In the other case, the spheroid was centrally masked with an equatorial screen, roughly simulating the colour effects of an embedded, optically thin, exponential disk of dust, also with $\epsilon$=0.74. As expected, *the effects upon the isochromes are strikingly different*, and offer some possibility of discrimination between the two options.

*A real galaxy* may well contain a disk *with both the above discussed characteristics*. This seems indeed to be the case in a number of strongly inclined S0 objects, according to our un-

**Table 1.** Characteristics of the $B-R$ distribution in flat diE. (1) Maximum ellipticity. (2) Range of isophotal radius, where a disk is well seen, i.e. $e_4 > .01$. (3) Importance of a local colour pattern. (4) Presence of a redder major axis. (5) Range of visibility of this feature. (6) Presence of the minor axis asymmetry. (7) Range of visibility of this feature. (8) Notes to Table 1.
(a) NGC821: Outer range perturbated by bright star, inner range by dust lane.
(b) NGC3377: A faint core colour pattern is superimposed.
(c) NGC3610: The disk dust layer is not symmetric along the major axis.
(d) NGC4564: Noisy data.
(e) NGC4660: Inner range perturbated by dust lane.
All ranges refer to the radius $r$ in arcsec. A colon: signals an uncertain result. A question mark ? indicates that the identification of the looked for feature is ambiguous.

| NGC | (1) | (2) | (3) | (4) | (5) | (6) | (7) | (8) |
|---|---|---|---|---|---|---|---|---|
| 0584 | 0.41 | 25-40 | 0 | yes | 12-30 | no: | - | - |
| 0821 | 0.39 | 3-26 | 1 | ? | - | ? | - | (a) |
| 3377 | 0.51 | 1-21 | 1- | ? | 1-7 | yes: | 1-5 | (b) |
| 3585 | 0.52 | 2-40 | 0 | yes | 1-30 | yes | 2-8 | - |
| 3610 | 0.43 | 1-8 | 0 | yes | 2-5 | yes | 2-5 | (c) |
| 4473 | 0.46 | 2-12 | 0 | yes | 1-10 | yes | - | - |
| 4564 | 0.40 | 9-29 | 1- | yes | 5-20 | ? | - | (d) |
| 4621 | 0.39 | 1-25 | 0 | yes | 1-10 | ? | - | - |
| 4660 | 0.44 | 8-50 | 1 | yes: | 5-15 | yes: | - | (e) |

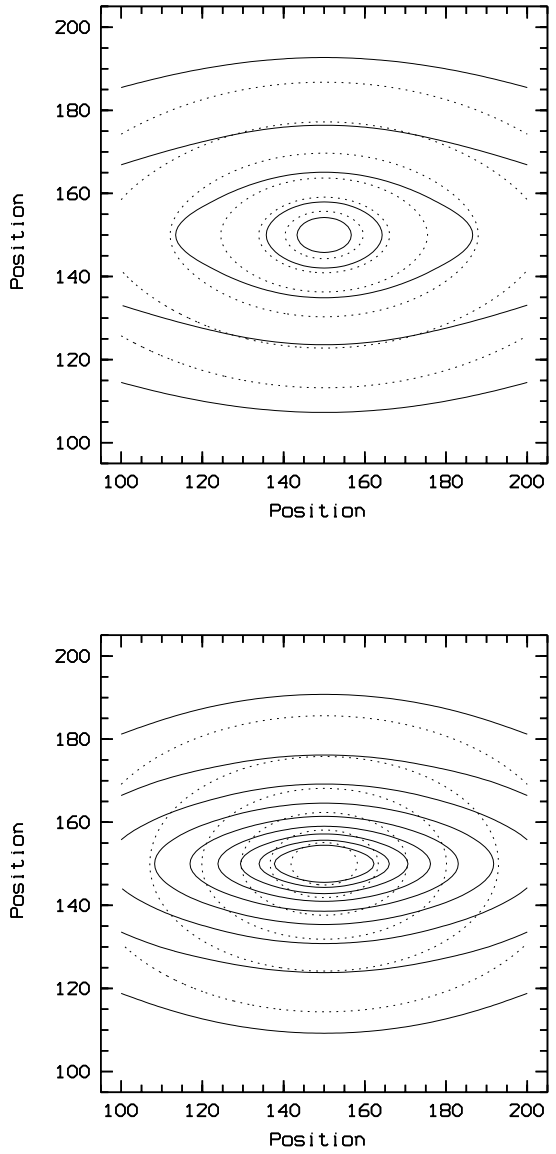


**Fig. 1.** Results of two numerical experiments briefly described in 3.1. The graphs compare the isochromes (full lines) and the isophotes (dotted lines). X,Y positions in arbitrary units. Upper graph: A model galaxy is made up of a spheroid with noticeable colour gradient and a disk of constant colour: the inner isochromes follow the isophotes of the spheroid, then become much flatter as the disk becomes influential. Lower graph: The spheroid contains a moderately flat, optically thin, exponential disk of dust. In this case the inner isochromes are much flatter than the isophotes.

published data with Dr. Poulain. Such a situation could perhaps be disentangled by a complex modelling, based upon a variety of colour and population data. For the time being, we consider *flat isochromes near the galaxian center as indicative of dust concentration in the disk*. The alternative hypothesis of a redder population throughout the disk is not retained, because several of the studied S0's show a relatively blue disk, as was found for NGC3115 by Silva et al. (1989).

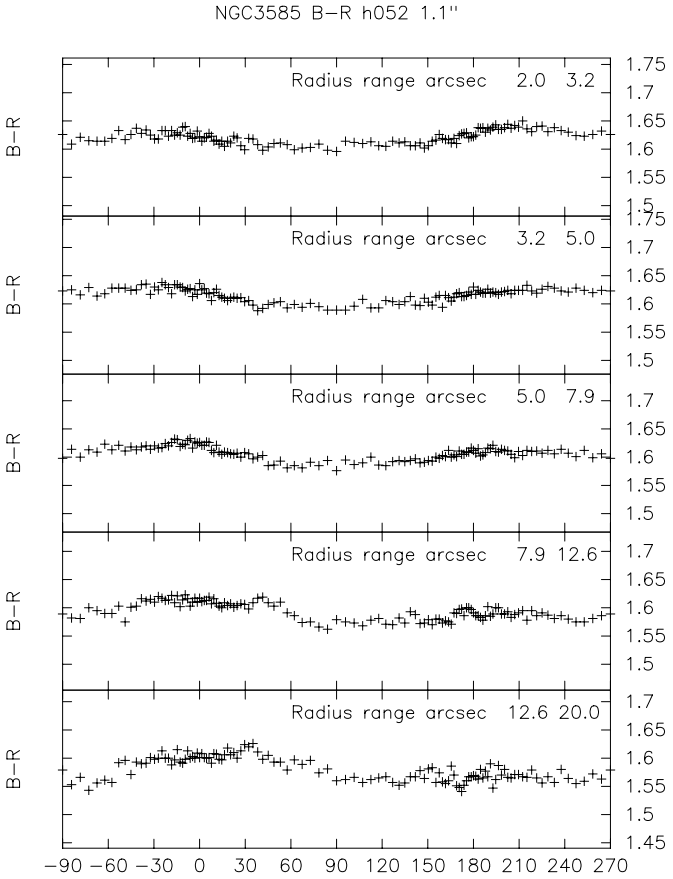


**Fig. 2.** Azimuthal $B-R$ distribution for the diE galaxy NGC3585 from CFHT observations. Abscissae: polar angle in degrees, with major axis at 0 and 180. Measurements are made at equal spacings in the eccentric anomaly $\omega$, producing unequal spacing in polar angle for flattened contours. Each curve is labelled with the limiting radii of each of the measured "isophotal rings". These graphs show the redder disk phenomenon in most of the measured "rings". The minor axis colour asymmetry is seen only in the 2 or 3 inner "rings". The tips of the major axis seem also to be of unequal colours.

### *3.2. The case of inclined normal diE's*

There are 13 diE galaxies in Nieto's sample, of such inclinations that it was thought useful to look for the kind of evidence for "dust in the disk" discussed above. From these candidates objects, NGC2768, 2974 and 4125 were discarded because they contain outstanding dust patterns, masking more subtle properties of the colour distribution (see Paper I of this series, Michard 1998a). NGC3613 was rejected because only short exposure noisy frames are available.

Table 1 lists the 9 remaining inclined diE's, E5 and flatter (except NGC0584), and the occurrence of the following characters: (1) irregular colour pattern; (2) redder major axis; (3) minor axis asymmetry.

Except for NGC821 and 3377 where ambiguities arise, all these objects show evidence for dust concentration towards their equatorial plane, or, otherwise stated, in their disk. Note the presence of a (rough) coincidence between the range of isophote radii where a disk is clearly seen from the $e_4$ harmonic coef-

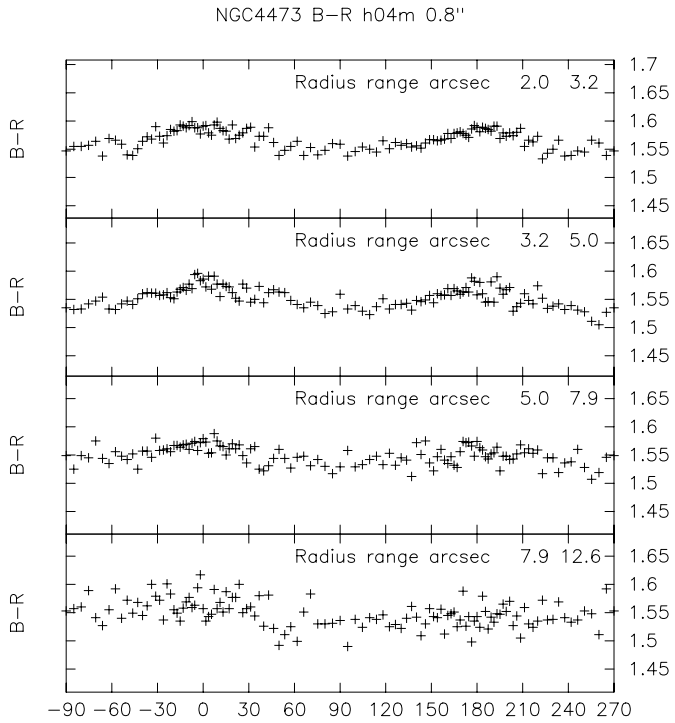


**Fig. 3.** Azimuthal $B-R$ distribution for the diE galaxy NGC4473 from CFHT observations. See the caption to Fig. 2 for explanations. In this case, the disk, and the associated colour enhancement, tend to disappear for $r > 10$ arcsec

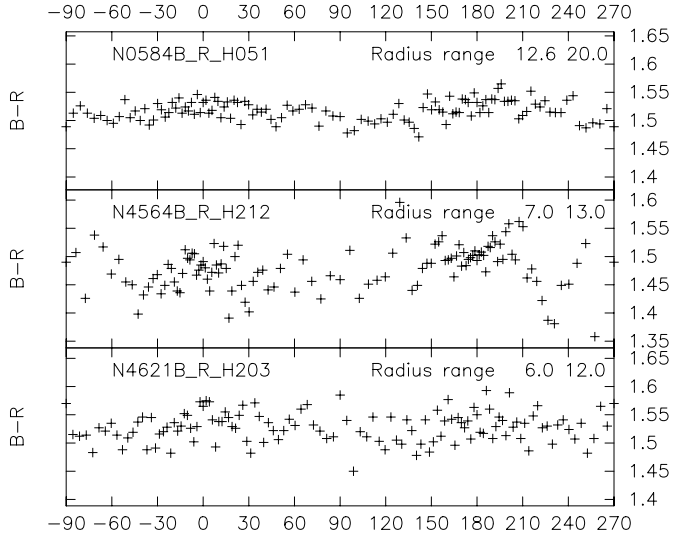


**Fig. 4.** Azimuthal $B-R$ distribution for selected "isophotal rings" in NGC0584, 4564 and 4621 from CFHT observations. In these cases, the major axis reddening is smaller than for the objects in Figs. 2 and 3, and barely exceeds noise in some cases.

ficient, and the range where the major axis is redder than the minor axis.

The "redder disk" phenomenon is presented in Fig. 2 for the diE galaxy NGC3585: it shows the azimuthal $B-R$ distribution in 5 "isophotal rings". The maximum of $B-R$ near polar angles 0 and 180 degrees is clearly seen. There is also evidence for a

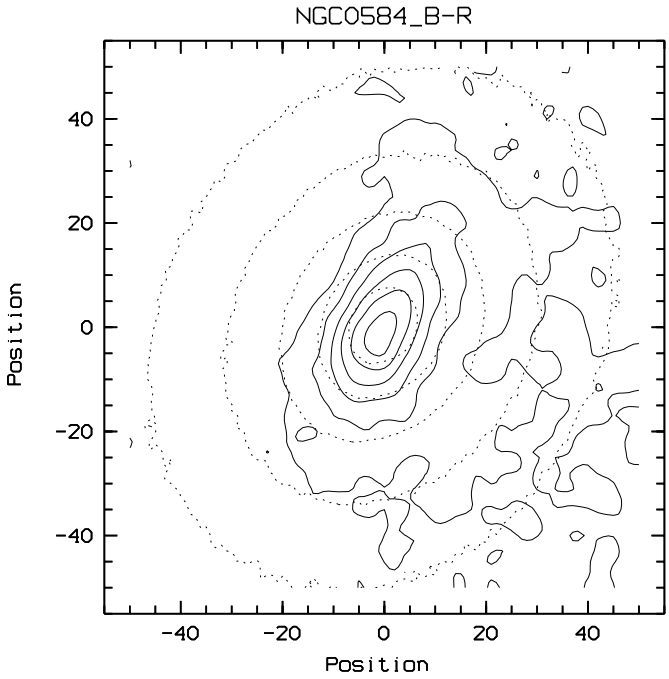


**Fig. 5.** Comparison of $B-R$ isochromes and B isophotes for NGC0584. Field 11.1x11.1 arcsec; N at 9 o'clock. Positions in pixels of 0.107 arcsec. $B-R$ contours (full): 1.475-1.60 (0.025). B contours (dotted): 17.0-19.0 (0.5) Note the flattening of the inner isochromes and possible minor axis asymmetry.

minor axis asymmetry in colour, with the side at polar angles near 90 slightly bluer than at -90 degrees, at least in two of the displayed "rings".

Fig. 3 shows a similar diagram for NGC4473. In this case, the disk is less extended, both from the $e_4$ profile and from the major axis reddening effect. Note that Goudfrooij et al. (1994b), find a blue disk in NGC4473 from $V-I$ data: this disagreement will be discussed in a forthcoming paper of this series dealing in detail with technical problems, notably the one of PSF's matching briefly mentioned above.

Fig. 4 gives the azimuthal $B-R$ distributions for 3 other diE's, in selected radial ranges of isophotal contours where the disk is well seen. In these cases the red disk phenomenon is small but definitely present. For NGC4564, OHP data of much better S/N ratio (but 2-3 arcsec seeing!) fully confirm the red disk effect.

Isochromes and isophotes are intercompared for such objects where the S/N ratio of our data is sufficient, that is NGC0584, 3377, 3585, 3610, 4473, 4621 and 4660, in Figs. 5 to 11. Note that the contour values are uncorrected for galactic and K effects. Most of these show flattened central isochromes, sometimes displaced and broadened on one side due to the minor axis asymmetry. It should be emphasized that NGC0584 is a diE with an inner "decoupled" disk (see below). It seems likely that the properties of the inner isochromes should be associated with dust in the inner disk, rather than in the "main" disk seen much farther according to Table 1. The disk reddening at larger

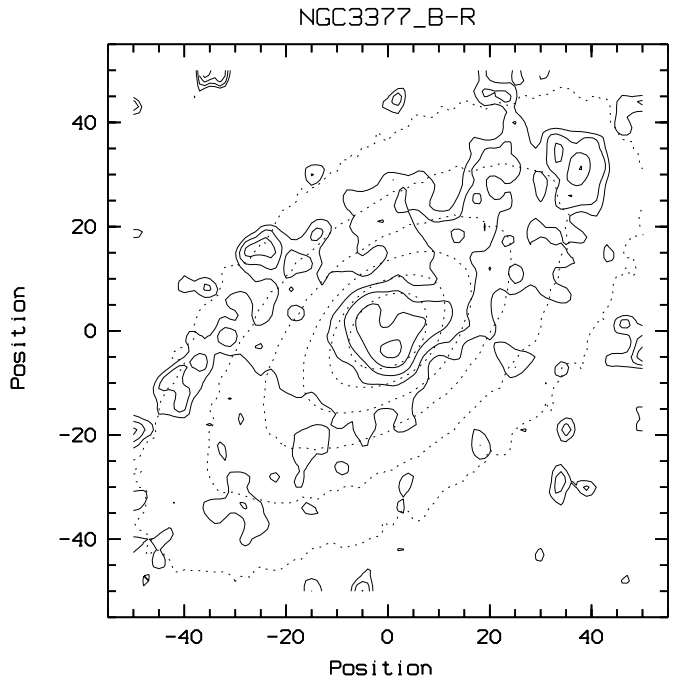


**Fig. 6.** Comparison of $B-R$ isochromes and B isophotes for NGC3377. Positions in pixels of 0.107 arcsec. Field 11.1x11.1 arcsec; N at 9 o'clock. $B-R$ contours (full): 1.50-1.60 (0.025). B contours (dotted): 17.0-19.0 (0.5) A lane on the N-W side may be due to dust in the disk, but the other criteria are quite uncertain.

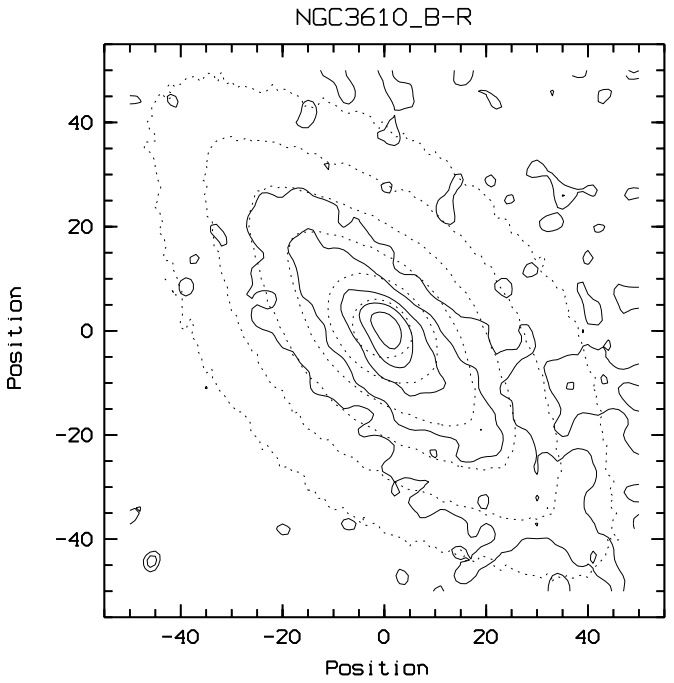


**Fig. 8.** Comparison of $B-R$ isochromes and B isophotes for NGC3610. Positions in pixels of 0.107 arcsec. Field 11.1x11.1 arcsec; N at 9 o'clock. $B-R$ contours (full): 1.475-1.575 (0.025). B contours (dotted): 16.75-19.25 (0.5) Note the flattening of the inner isochromes and a clear minor axis asymmetry.

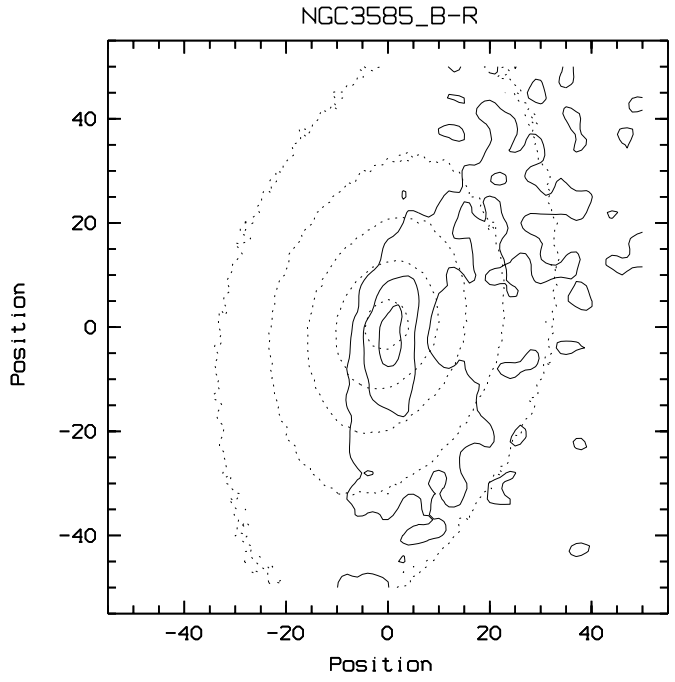


**Fig. 7.** Comparison of $B-R$ isochromes and B isophotes for NGC3585. Positions in pixels of 0.107 arcsec. Field 11.1x11.1 arcsec; N at 9 o'clock. $B-R$ contours (full): 1.63-1.68 (0.025). B contours (dotted): 16.5-18.5 (0.5) Note the flattening of the inner isochromes and a clear minor axis asymmetry.

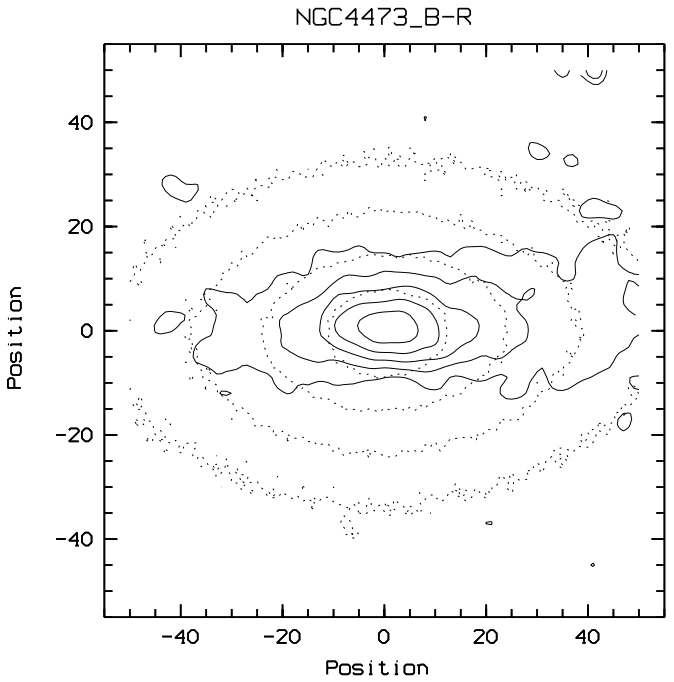


**Fig. 9.** Comparison of $B-R$ isochromes and B isophotes for NGC4473. Positions in pixels of 0.107 arcsec. Field 11.1x11.1 arcsec; N at 12 o'clock. $B-R$ contours (full): 1.575-1.675 (0.025). B contours (dotted): 16.75-18.75 (0.5) Note the flattening of the inner isochromes and possible minor axis asymmetry.

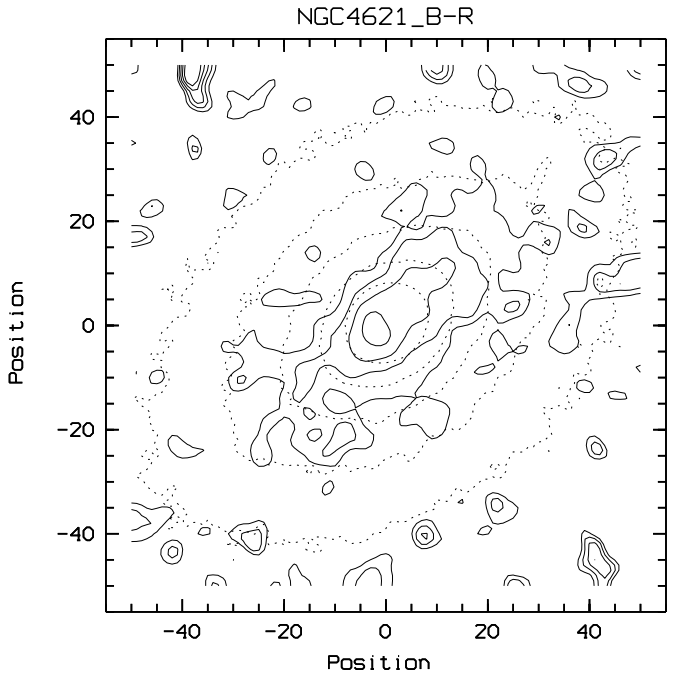


**Fig. 10.** Comparison of $B-R$ isochromes and B isophotes for NGC4621. Positions in pixels of 0.107 arcsec. Field 11.1x11.1 arcsec; N near 7 o'clock. $B-R$ contours (full): 1.59-1.69 (0.025). B contours (dotted): 16.75-18.75 (0.5) Note the flattening of the inner isochromes and possible minor axis asymmetry

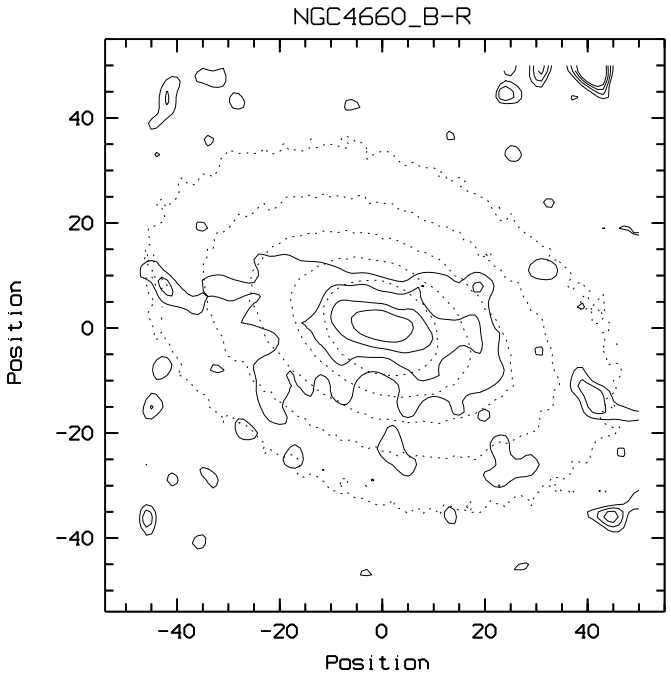


**Fig. 11.** Comparison of $B-R$ isochromes and B isophotes for NGC4660. Positions in pixels of 0.107 arcsec. Field 11.1x11.1 arcsec; N near 1 o'clock. $B-R$ contours (full): 1.55-1.65 (0.025). B contours (dotted): 17.0-19.0 (0.5) Note the flattening of the inner isochromes, and a dust pattern slightly tilted from the major axis.

radii shown in Fig. 4 may be due to dust in the main disk, but this remains uncertain.

As regards NGC3377, the HST frame published in Lauer et al. (1995) should be examined. It shows a dust arc rougly parallel but away from the major axis. This feature is also present in our data and prevents an unambiguous identification of disk reddening. A worse difficulty occurs for NGC0821 with an inner minor axis dust lane.

*From the above evidence, it is sugested that dust is often present in the disks of diE's: this is also true even as no such pattern as patches or lanes are seen, as is the case for most of the above discussed objects*. It seems however likely, from the smaller major axis colour contrast observed in diE's as compared to S0's (unpublished data by Michard and Poulain), that the amount of dust is distinctly smaller in the former case.

### *3.3. Galaxies with inner disks near the core*

Some E galaxies, including boE's, show an *inner disk* seemingly "decoupled" from the main morphological structure of the object, as Nieto et al. (1991a) pointed out. Such features are easily detected in the CFHT data from a well separated inner maximum in the $e_4$ profile; this should be associated with a local maximum of $\epsilon$ (or at least a significant plateau) to make the case convincing.

The profile of the $e_4$ coefficient is given in Fig. 9 for the 7 galaxies of the sample showing such an inner disk: 3 are boE's while 3 are diE where the main disk is well separated from the inner one. The subclass of NGC4494 is unE.

**Table 2.** E galaxies with inner decoupled disks.
(1) major axis range of the inner disk from thr $e_4$ profile (arcsec). (2) Maximum ellipticity associated with the inner disk. (3) Morphology of main galaxian body, diE, boE or unE. (4) major axis range for this morphology. (5) Evidence for a redder colour of the inner disk. (6) Notes to Table 5:
(a) Doubtful due to relatively poor resolution.
(b) Doubtful due to poor S/N.
(c) Doubtful due to the occurrence of an irregular core colour pattern.
The symbol ? indicates a doubtful case

| NGC | (1) | (2) | (3) | (4) | (5) | Notes |
|---|---|---|---|---|---|---|
| 0584 | 0.5-3 | 0.24 | diE | $>30$ | yes | (a) |
| 4478 | 1-4 | 0.26 | boE | $>5$ | no | - |
| 4494 | 2-6 | 0.21 | unE | $>10$ | no | - |
| 4551 | 0.6-3 | 0.30 | boE | $>4$ | no | (b) |
| 5322 | 1.5-6 | 0.39 | boE | $>10$ | yes | - |
| 5831 | 0.7-3 | 0.30 | diE | $>9$ | yes? | (c) |
| 5845 | 0.7-3 | 0.37 | diE | $>9$ | yes | - |

Table 2 presents our evaluation of the possibility of dust concentration in the inner disk of these 7 objects. The criteria in this evaluation are, as above for the flatter diE, the relative reddening of the major axis and eventually the minor axis asymmetry.

The detection of a detail in the colour distribution unambigously associated with the small inner disk of this class of objects is difficult. It may be noted that the success and relia-

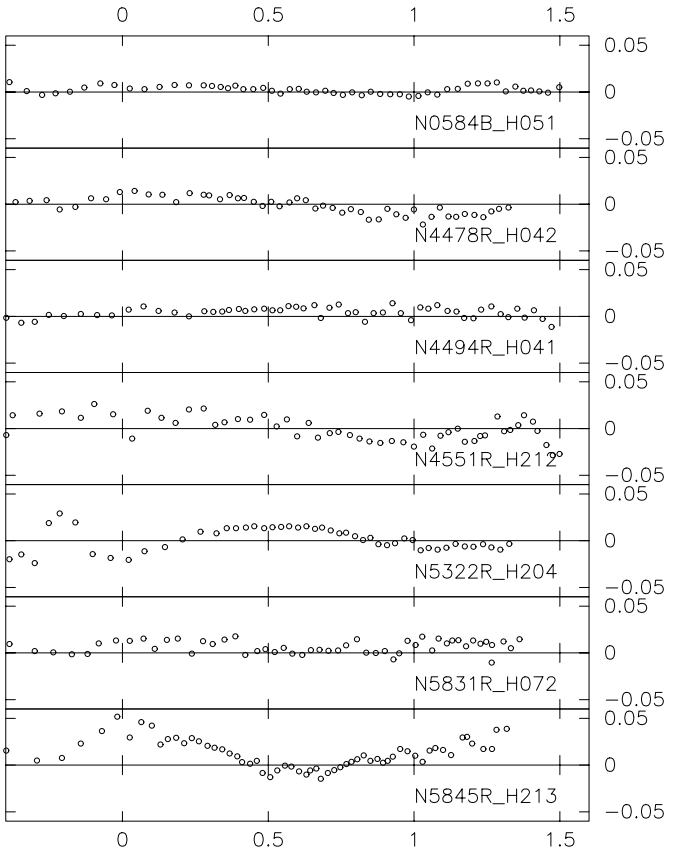


**Fig. 12.** The $e_4$ coefficient for 7 galaxies showing evidence of an inner "decoupled" disk, from R frames of the Nieto sample. Abscissae: logarithm of the major axis $a$ in arcsec. NGC4478, 4551 and 5322 are boxy at larger $a$ values. NGC4494 is classified unE while the other are disky.

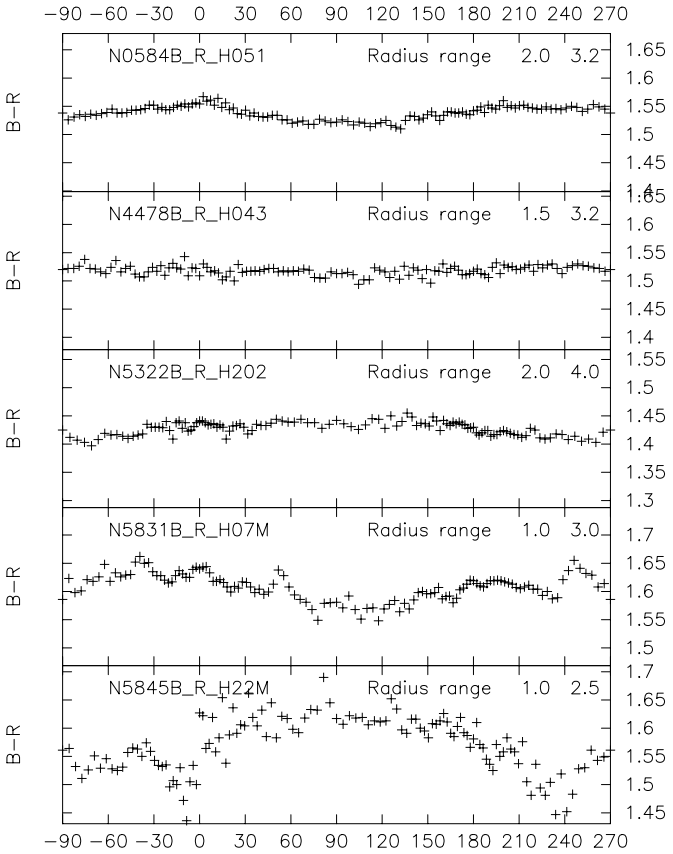


**Fig. 13.** Azimuthal $B-R$ distributions in "isophotal rings" intercepting the inner "decoupled" disks of 4 objects showing some evidence of dust concentration in this disk. NGC4478 is shown for comparison as an object with an inner disk but without associated colour effect.

bility of the detection is correlated with the inclination of the disk as indicated by the associated local value of $\epsilon$. Fig. 10 shows the $B-R$ azimuthal distribution in an inner "isophotal ring" intercepting the inner disk, for the objects with some evidence of dust in their inner disk. As a comparison, the case of NGC4478, with an inner disk but no associated colour effect is also shown. The minor axis asymmetry is present in the inner colour distributions of NGC0584, 5322, 5831, 5845.

HST images of two of the present objects, i.e. NGC5322 and 5845 are displayed in Lauer et al. (1995). These show the inner disks, associated dust arclets and even the induced minor axis asymmetry... much better than our present diagrams! The very thin dust layers in the inner disks are not resolved in our frames. In the same atlas of HST images, NGC4551 shows no dust, while NGC4697 (not in our sample) has a dust arc associated with its inner stellar disk.

## 4. Discussion and conclusion

In Paper I of this series, a strong correlation was found between the presence of a disk in E galaxies, and the presence of a dust pattern, i.e. patches, lanes, arcs..., detected from local reddening: in other words, diE's are much more likely to show a dust pattern than boE's. It is now suggested that *the modest disks of E galaxies normally contain some dust, even as no local features are seen*, at least at the resolution of our data.

The main evidence lies in the reddening observed along the major axis of flattened ellipticals, as compared to the corresponding minor axis of an isophote. For an oblate object, a line of sight through the major axis integrates more light from the equatorial layer than other lines of sight, so that a redder major axis is expected whenever dust is concentrated towards the equator, notably when the dust lies in a thin layer in coincidence with a stellar disk. If this layer is extended and thick enough, it may produce a different extinction and reddening on both sides of the bulge, i.e. the "minor axis asymmetry" documented for S0's in MS93. The redder major axis is a somewhat ambiguous evidence, as discussed in 3.1, but the ambiguity can be solved with some degree of confidence.

One of these properties, or both, are observed in 8 diE's of maximum ellipticities in the range $0.39 < \epsilon < 0.52$, including 2 where a dust arc appears somewhat displaced from the major axis, but is likely to lie in the disk. The 3 other objects of such geometry in our sample also contain dust in large patterns, but no association with the disk is apparent. *It seems therefore that the "dust in the disk" phenomemon is quite frequent in the main disk of diE's.*

This may also be true for the innermost "decoupled" disks occurring in both boE's and diE's. This finding is only rather marginal in our data, but HST images of two objects with such an inner disk, i.e. NGC5322 and 5845 indeed show the associated dust layer.

The present observations suggest that more effort to modelize "diffuse" dust in E-S0 galaxies would be useful. The present models for spherical systems are clearly inadequate for disky E's. Models with a thin dust layer embedded in the stellar disk (see MS93) would be a natural first approximation to describe this class of objects.

In Paper I of this series, it was found that dust "patterns" avoid boE's, while they appear in the majority of diE's and in about half unE's. It is now found that dust is often present in or near the disk of other diE's, without forming a distinct pattern, and also in "decoupled" inner disks. It may be hoped that this association of dust with stellar disks will be of interest for the current discussion of the formation and evolution of "hot" galaxies. It should be emphasized that this association is not extremely tight: there are E-S0's disky galaxies where no dust is optically detected; there are also diE's or unE's galaxies where the dust appears in a pattern without relation to the disk (or at least to the major axis).

*Acknowledgements.* I am indebted to my colleagues at the Observatoire du Midi-Pyrénées, Dr. E. Davoust and P. Poulain who put at my disposal the frames of the "Nieto sample". I thank the referee for very helpful criticisms.

## References

Carter, D., 1978, MNRAS 182, 797
Franx, M., Illingworth, G., Heckman, T., 1989, AJ 98, 538
Goudfrooij, P., Hansen, L., Jorgensen, H.E., et al., 1994a, A&AS 104, 179
Goudfrooij, P., Hansen, L., Jorgensen, H.E., et al., 1994b, A&AS 105, 341
Goudfrooij, P., de Jong, T., 1995, A&A 298, 784
Goudfrooij, P., 1995, Messenger 79, 31
Hansen, L., Norgaard-Nielsen, H.U., Jorgensen, H.E., 1991, A&A 243, 49
de Jong, T., Norgaard-Nielsen, H.U., Hansen, L., et al., A&A 232, 317
Jura, M., 1978, ApJ 223, 421
Jura M., Kim, D.W., Knapp, G.R., Guha tha Kurta, P., 1987, ApJL 312, L11
Knapp, G.R., Guha tha Kurta, P., Kim, D.W., Jura, M., 1989, ApJS 70, 329
Lauer, T.R., Ajhar, E.A., Byun, Y.I. et al., 1995, AJ 110, 2622
Michard, R., 1994, A&A 288, 401
Michard, R., 1998a, A&A in press
Michard, R., Marchal, J., 1991, A&A 243, 103
Michard, R., Marchal, J., 1994, A&AS 105, 81
Michard, R., Simien, F., 1993, A&A 274, L25 (MS93)
Nieto, J.L., Bender, R., Arnaud, J., Surma, P., 1991a, A&A 244, L25
Nieto, J.L., Bender, R., Surma, P., 1991b, A&A 244, L37
Peletier, R.F., Davies, R.L., Illingworth, G.D., Davis, L.E., Cawson, M., 1990, AJ 100, 1091
Silva, D.R., Boroson, T.A., Thompson, I.B., Jedrzejewski, R.I., 1989, AJ 98, 131
Silva, D.R., Wise, M.J., 1995, in Fresh Views of Elliptical galaxies, Proc. INAOE Int. Meet., Puebla, Mex., 14-17/3/95
Vigroux, L., Souviron, J., Lachieze-Rey, M., Vader, J.P., 1988, A&AS 73, 1
Wise, M.J., Silva, D.R., 1996, ApJ 461, 155
Witt, A., Thronson, H.A.jr, Capuano, J.M., 1992, ApJ 393, 611